Huang *et al. BMC Pulmonary Medicine* (2025) 25:99
https://doi.org/10.1186/s12890-025-03559-3

BMC Pulmonary Medicine

RESEARCH

Open Access

Predictors of occult lymph node metastasis in clinical T1 lung adenocarcinoma: a retrospective dual-center study

Xiaoxin Huang[1], Xiaoxiao Huang[2], Kui Wang[1], Lijuan Liu[1] and Guanqiao Jin[1*]

Abstract

Background The optimal surgical strategy for lymph node dissection in lung adenocarcinoma remains controversial. Accurate predicting occult lymph node metastasis (OLNM) in patients with clinical T1 lung adenocarcinoma is essential for optimizing treatment decisions and improving patient outcomes. This study analyzes the relationship between anaplastic lymphoma kinase (*ALK*) status, clinicopathological characteristics, computed tomography (CT) features, and OLNM in patients with clinical T1 lung adenocarcinoma.

Methods A retrospective analysis was conducted on data from patients with clinical T1 lung adenocarcinoma who showed no lymph node metastasis on preoperative CT and underwent surgical resection with lymph node dissection at two centers from January 2016 to December 2023. Univariate and multivariate logistic regression analyses were performed to identify factors associated with OLNM.

Results Among 1138 patients with clinical T1 lung adenocarcinoma, 167 (14.6%) were found to have OLNM, including 55 (4.8%) with pathological N1 status and 112 (9.8%) with pathological N2 status. Multivariate logistic regression analysis identified lobulation, spiculation, solid density, lymphovascular invasion, spread through air spaces (STAS), micropapillary pattern, solid pattern, and carcinoembryonic antigen (CEA) levels as independent positive predictors of OLNM. Furthermore, lobulation, lymphovascular invasion, STAS, micropapillary pattern, solid pattern, CEA levels, and *ALK* were independent positive predictors of occult N2 lymph node metastasis. The lepidic pattern, however, was identified as an independent negative predictor for OLNM and occult N2 lymph node metastasis.

Conclusion The identified predictors may assist clinicians in evaluating the risk of OLNM in patients with clinical T1 lung adenocarcinoma, potentially guiding more targeted intervention strategies.

Keywords Lung adenocarcinoma, Occult lymph node metastasis, Predictor, Anaplastic lymphoma kinase

*Correspondence:
Guanqiao Jin
jinguanqiao77@gxmu.edu.cn
[1]Guangxi Medical University Cancer Hospital, Nanning 530021, Guangxi, China
[2]Affiliated Hospital of Youjiang Medical University for Nationalities, Baise 533000, Guangxi, China

Introduction

According to the latest estimates from the International Agency for Research on Cancer, lung cancer remains the most prevalent cancer globally, accounting for 12.4% of all cancer cases, and it is also the leading cause of cancer-related mortality [1]. With the increased use of computed tomography (CT) imaging, more lung cancers are now being detected at an early stage. Consequently, the incidence of advanced-stage lung cancer has declined, while the incidence of localized-stage lung cancer is increasing each year [2]. Surgical resection remains the primary treatment modality for early-stage lung cancer [3]. Adenocarcinoma, the most prevalent histological subtype of non-small cell lung cancer (NSCLC), has a prognosis that is primarily determined by the stage of the tumor. However, accurate preoperative lymph node staging remains challenging, as CT and positron emission tomography/computed tomography (PET/CT) scans show limited sensitivity in detecting mediastinal lymph node metastasis [4]. Thus, obtaining precise preoperative N staging is crucial for guiding treatment decisions and predicting outcomes in patients with lung adenocarcinoma.

Several clinical factors have been linked to lymph node metastasis in lung adenocarcinoma, including age [5], consolidation-to-tumor ratio [6], depth ratio [7], smoking status [6], gender [7], tumor size [6, 8], tumor location [9], and preoperative carcinoembryonic antigen (CEA) level [6, 8]. Additionally, Cytokeratin fragment 19 (CYFRA21-1) may help predict mediastinal lymph node metastasis in lung cancer [10], and carcinoma antigen 125 (CA125) has been suggested as a potential marker for occult lymph node metastasis (OLNM) in NSCLC [11, 12]. Pathological features, such as micropapillary and solid patterns, have been associated with occult N2 lymph node metastasis [10, 11]. Moreover, pleural invasion and lymphovascular invasion correlate with lobar lymph node metastasis in non-primary tumor-bearing lobes of NSCLC [12], radiological signs like pleural indention and the nonvascular penetration sign may predict lymph node metastasis in T1 lung adenocarcinoma [7]. Anaplastic lymphoma kinase (*ALK*) rearrangement has also been associated with OLNM in lung adenocarcinoma and is considered a risk factor for postoperative recurrence in early-stage disease [13, 14]. However, few studies have integrated *ALK* gene expression with CT features and clinicopathological characteristics to predict OLNM in T1 lung adenocarcinoma. Furthermore, the need for lymph node dissection in early-stage lung adenocarcinoma remains controversial, particularly in patients considered to have a low risk of metastasis. Accurately identifying patients at risk of OLNM could help refine treatment strategies and improve patient outcomes. In this retrospective study, we investigated the incidence and predictors of OLNM in clinical T1 lung adenocarcinoma, aiming to provide data that may assist clinicians in risk stratification and therapeutic decision-making.

Materials and methods

Patients

This study was approved by the institutional review board of our institution, with a waiver of informed consent due to its retrospective nature. We retrospectively analyzed clinical data from patients at Guangxi Medical University Cancer Hospital and the Affiliated Hospital Youjiang Medical College for Nationalities, who underwent surgical resection combined with lymph node dissection and were pathologically diagnosed with lung adenocarcinoma from January 2016 to December 2023. The inclusion criteria were as follows: (1) The clinical N stage before the operation should be N0 and the maximum tumor diameter on the CT image should be 3 cm or less; (2) The pathology was confirmed as lung adenocarcinoma; (3) lobectomy, wedge resection, or segmentectomy combined with lymph node dissection was performed. Exclusion criteria included: (1) patients who received neoadjuvant therapy; (2) carcinoma in situ; (3) incomplete clinical data; (4) lack of systematic lymph node dissection or sampling during surgery. Clinical stage N0 was defined based on CT scans, indicating the absence of hilar or mediastinal lymph node enlargement, with lymph nodes measuring less than 1 cm in their shortest axis diameter. Systematic lymph node dissection was defined as the removal of at least three mediastinal lymph node stations, including the subcarinal station when applicable, along with all hilar and intrapulmonary lymph nodes on the ipsilateral side. Systematic lymph node sampling, by contrast, involved the targeted removal of specific lymph node stations as predetermined by the surgeon [15]. A total of 1138 patients were included in the study. Clinical data collected included age, gender, smoking history, *ALK* (D5F3 Ventana) rearrangement status, preoperative levels of CYFRA21-1, CEA, and CA125, as well as the type of surgery performed. TNM staging was determined according to the 8th edition guidelines of the Inter-National Association for the Study of Lung Cancer.

All surgical specimens were examined by pathologists whose observations were recorded. Each pathology report was reviewed for lymph node status, emphysema, visceral pleural invasion, perineural invasion, lymphovascular invasion, and spread through air spaces (STAS), and pathological subtypes of adenocarcinoma (lepidic, acinar, papillary, micropapillary, solid, complex glandular, cribriform). The IASLC/ATS/ERS lung adenocarcinoma classification system was applied. The percentage of each histological component was recorded in 5% increments, and tumors were classified according to the predominant pattern. The pattern was considered present if ≥ 5% of the histological pattern was present in the tumor.

The CT features of the tumor were interpreted by two radiologists (with 20 and 9 years of experience in thoracic imaging diagnosis), who were blinded to the related clinicopathological data. In case of any differences, decisions were reached by consensus. The following CT features of tumors were measured and analyzed: tumor size (maximum diameter), density (solid, part solid, ground-glass opacity [GGO]), tumor lobe (right upper lobe, right middle lobe, right lower lobe, left upper lobe, left lower lobe), location (central, peripheral), lobulation, spiculation, pleural indentation, air bronchogram, vascular cluster, vacuole, and emphysema.

Statistical analysis

Continuous variables with a normal distribution were presented as the mean ± standard deviation. Skewed data were reported as the median with interquartile ranges (median [Q1, Q3]). Categorical variables were expressed as frequencies and percentages. To investigate the association between variables and lymph node metastasis, univariate binary logistic regression analyses were first conducted. Variables that were statistically significant in the univariate analyses were subsequently included in multivariate binary logistic regression analyses. The diagnostic performance of the model was evaluated by calculating the area under the receiver operating characteristic curve (AUC), along with the sensitivity and specificity. All data were performed with the SPSS software (version 22; IBM, USA). A two-sided $P < 0.05$ was considered statistically significant.

Results

In the study, we included 460 (40.4%) men and 678 (59.6%) women. The median age was 58 years (interquartile range [IQR]: 51, 65). 1136 (99.8%) patients had tumors located at the periphery. 229 (20.1%) patients were smokers. The majority of tumors were located in the right upper lobe (369 patients, 32.4%), while the fewest were in the right middle lobe (111 patients, 9.8%). OLNM was observed in 167 (14.7%) patients, with 55 (32.9%) having pathological N1 status and 112 (67.1%) having pathological N2 status. No lymph node metastasis was detected in the GGO group. The median tumor maximum diameter was 16.5 mm (IQR: 12, 22). Among all patients, 638 (56.0%) underwent lobectomy, 375 (33.0%) underwent wedge resection and 125 (11.0%) underwent segmentectomy. The detailed variables of the patients are listed in Table 1.

Predictors of occult lymph node metastasis

The results of the univariate analysis of OLNM in patients with clinical T1 lung adenocarcinoma are presented in Table 2. Patient age, gender, location of the tumor (central and peripheral), lung lobes, air bronchogram, complex glandular pattern, emphysema, and CYFRA21-1 did not differ significantly between the pathological N0 and pathological N1 + N2 groups. Factors significantly associated with OLNM included smoking history ((odds ratio [OR] = 1.891, $p < 0.001$), tumor maximum diameter (OR = 1.129, $p < 0.001$), density (OR = 0.116, $p < 0.001$), lobulation (OR = 47.179, $p < 0.001$), spiculation (OR = 6.762, $p < 0.001$), pleural indentation (OR = 4.605, $p < 0.001$), vascular cluster sign (OR = 2.791, $p < 0.001$), vacuole (OR = 2.190, $p < 0.001$), lepidic pattern (OR = 0.214, $p < 0.001$), acinar pattern (OR = 2.516, $p < 0.001$), papillary pattern (OR = 1.483, $p = 0.020$), micropapillary pattern (OR = 4.895, $p < 0.001$), solid pattern (OR = 6.885, $p < 0.001$), cribriform pattern (OR = 5.266, $p = 0.002$), predominant pattern (OR = 1.843, $p < 0.001$), visceral pleural invasion (OR = 2.835, $p < 0.001$), perineural invasion (OR = 9.023, $p < 0.001$), lymphovascular invasion (OR = 9.668, $p < 0.001$), STAS (OR = 7.320, $p < 0.001$), *ALK* (OR = 4.221, $p < 0.001$), CEA (OR = 3.443, $p < 0.001$), CA125 (OR = 2.930, $p = 0.002$). Multivariate logistic regression analysis revealed that lobulation (OR = 11.083, $p < 0.001$), spiculation (OR = 1.638, $p = 0.045$), lymphovascular invasion (OR = 2.969, $p < 0.001$), STAS (OR = 2.280, $p < 0.001$), micropapillary pattern (OR = 2.222, $p = 0.001$), solid pattern (OR = 2.681, $p < 0.001$), CEA (OR = 1.702, $p = 0.029$) were identified as independent predictors associated with an increased risk of OLNM. Conversely, part solid density (OR = 0.379, $p = 0.004$) and lepidic pattern (OR = 0.578, $p = 0.031$) were independent predictors associated with a decreased risk of OLNM. Specifically, the association of part solid density indicated that solid density was linked to a higher risk of OLNM. The results of multivariate logistic regression analyses of OLNM are shown in Table 3; Fig. 1.

The ability of each factor to predict OLNM on its own was not conclusive. However, integrating nine independent predictive factors (lobulation, speculation, density, lymphovascular invasion, STAS, lepidic pattern, micropapillary pattern, solid pattern, and CEA) into the multivariate logistic regression equation yielded more inclusive probability values. Then, we generated a receiver operating characteristic curve (ROC) to predict OLNM (Fig. 2). The AUC was 0.916 ($p < 0.001$, 95% CI 0.898–0.934), indicating a high diagnostic value.

Predictors of occult N2 lymph node metastasis

The results of the univariate analysis of occult N2 lymph node metastasis in patients with clinical T1 lung adenocarcinoma are shown in Table 2. Patient age, gender, location of the tumor (central and peripheral), lung lobes, air bronchogram, papillary pattern, complex glandular pattern, emphysema, and CYFRA21-1 did not differ

Table 1 Clinical, molecular, radiological, and pathological features distribution in the study population

Variables	All patients No. (%) (n = 1138)	pN0 No. (%) (n = 971)	pN1 + N2 No. (%) (n = 167)	pN2 No. (%) (n = 112)
Age (years)[a]	58(51,65)	58(51,65)	58(50,64)	58(51,64)
Gender				
Male	460(40.4)	381(39.2)	79(47.3)	52(46.4)
Female	678(59.6)	590(60.8)	88(52.7)	60(53.6)
Smoking history				
No	909(79.9)	792(81.6)	79(47.3)	81(72.3)
Yes	229(20.1)	179(18.4)	88(52.7)	31(27.7)
Maximum diameter (mm)[a]	16.5(12,22)	15(11,21)	21(17,25)	20(17,24)
Operation type				
Segmentectomy	125(11.0)	121(12.5)	4(2.4)	3(2.7)
Wedge resection	375(33.0)	337(34.7)	38(22.8)	29(25.9)
Lobectomy	638(56.0)	513(52.8)	125(74.9)	80(71.4)
Density				
Solid	548(48.2)	393(40.5)	155(92.8)	102(91.1)
Part solid	275(24.2)	263(27.1)	12(7.2)	10(8.9)
GGO	315(27.6)	315(32.4)	0(0)	0(0)
Location				
Central	2(0.2)	1(0.1)	1(0.6)	1(0.9)
Peripheral	1136(99.8)	970(99.9)	166(99.4)	111(99.1)
Lung lobes				
RUL	369(32.4)	314(32.3)	55(32.9)	39(34.8)
RML	111(9.8)	90(9.3)	21(12.6)	13(11.6)
RLL	216(20.0)	177(18.2)	39(23.3)	25(22.3)
LUL	259(22.7)	235(24.2)	24(14.4)	15(13.4)
LLL	183(16.1)	155(16.0)	28(16.8)	20(17.9)
Lobulation				
Absent	525(46.1)	521(63.7)	49(29.3)	35(31.2)
Present	613(53.9)	255(26.3)	118(70.7)	77(68.8)
Spiculation				
Absent	765(67.2)	716(73.7)	49(29.3)	35(31.2)
Present	373(32.8)	255(26.3)	118(70.7)	77(68.8)
Pleural indentation				
Absent	664(58.3)	618(63.6)	46(27.5)	32(28.6)
Present	474(41.7)	353(36.4)	121(72.5)	80(71.4)
Air bronchogram				
Absent	786(69.1)	673(69.3)	113(67.7)	81(72.3)
Present	352(30.9)	298(30.7)	54(32.3)	31(27.7)
Vascular cluster sign				
Absent	1041(91.5)	903(93.0)	138(82.6)	95(84.8)
Present	97(8.5)	68(7.0)	29(17.4)	17(15.2)
Vacuole				
Absent	939(82.5)	820(84.4)	119(71.3)	78(69.6)
Present	199(17.5)	151(15.6)	48(28.7)	34(30.4)
Lepidic pattern				
Absent	520(45.7)	393(40.5)	127(76.0)	88(78.6)
Present	618(54.3)	578(59.5)	40(24.0)	24(21.4)
Acinar pattern				
Absent	279(24.5)	258(26.6)	21(12.6)	11(9.8)
Present	859(75.5)	713(73.4)	146(87.4)	101(90.2)
Papillary pattern				
Absent	565(49.6)	496(51.1)	69(41.3)	47(42.0)
Present	573(50.4)	475(48.9)	98(58.7)	65(58.0)
Micropapillary pattern				
Absent	870(76.4)	791(81.5)	79(47.3)	53(47.3)
Present	268(23.6)	180(18.5)	88(52.7)	59(52.7)

Table 1 (continued)

Variables	All patients No. (%) (*n* = 1138)	pN0 No. (%) (*n* = 971)	pN1 + N2 No. (%) (*n* = 167)	pN2 No. (%) (*n* = 112)
Solid pattern				
Absent	947(83.2)	859(88.5)	88(52.7)	52(46.4)
Present	191(16.8)	112(11.5)	79(47.3)	60(53.6)
Complex glandular pattern				
Absent	1117(98.2)	955(98.4)	162(97.0)	108(96.4)
Present	21(1.8)	16(1.6)	5(3.0)	4(3.6)
Cribriform pattern				
Absent	1123(98.7)	963(99.2)	160(95.8)	107(95.5)
Present	15(1.3)	8(0.8)	7(4.2)	5(4.5)
Predominant pattern				
Lepidic predominant	332(29.2)	325(33.5)	7(4.2)	4(3.6)
Acinar predominant	505(44.4)	417(43.0)	88(52.7)	61(54.5)
Papillary predominant	196(17.2)	170(17.5)	26(15.6)	12(10.7)
Micropapillary predominant	27(2.4)	15(1.5)	12(7.2)	9(8.0)
Solid predominant	73(6.4)	40(4.1)	33(19.7)	25(22.3)
Complex glandular predominant	5(0.4)	4(0.4)	1(0.6)	1(0.9)
Visceral pleural invasion				
Absent	871(76.5)	774(79.7)	97(58.1)	68(60.7)
Present	267(23.5)	197(20.3)	70(41.9)	44(39.3)
Perineural invasion				
Absent	1116(98.1)	962(99.1)	154(92.2)	105(93.7)
Present	22(1.9)	9(0.9)	13(7.8)	7(6.3)
Lymphovascular invasion				
Absent	998(87.7)	902(92.9)	96(57.5)	66(58.9)
Present	140(12.3)	69(7.1)	71(42.5)	46(41.1)
STAS				
Absent	929(81.6)	848(87.3)	81(48.5)	57(50.9)
Present	209(18.4)	123(12.7)	86(51.5)	55(49.1)
Emphysema				
Absent	740(65.0)	633(65.2)	107(64.1)	72(64.3)
Present	398(35.0)	338(34.8)	60(35.9)	40(35.7)
ALK (D5F3 Ventana)				
Negative	1085(95.3)	939(96.7)	146(87.4)	92(82.1)
Positive	53(4.7)	32(3.3)	21(12.6)	20(17.9)
CYFRA21-1 (ng/ml)				
≤ 3.3	68(6.0)	56(5.8)	12(7.2)	103(92.0)
> 3.3	1070(94.0)	915(94.2)	155(92.8)	9(8.0)
CEA (ng/ml)				
< 5	1046(91.9)	914(94.1)	132(79.0)	84(75.0)
5–20	73(6.4)	51(5.3)	22(13.2)	19(17.0)
> 20	19(1.7)	6(0.6)	13(7.8)	9(8.0)
CA125 (U/mL)				
< 35	1101(96.7)	946(97.4)	155(92.8)	101(90.2)
≥ 35	37(3.3)	25(2.6)	12(7.2)	11(9.8)

Abbreviations: RUL, right upper lobe; RML, right middle lobe; RLL, right lower lobe; LUL, left upper lobe; LLL, left lower lobe; STAS, spread through air space; *ALK*, anaplastic lymphoma kinase; Cyfra21-1, cytokeratin 19-fragments; CEA, carcinoembryonic antigen; CA125, carcinoma antigen 125

[a] The data are the median, and the upper and lower interquartile ranges are in brackets

significantly between the pathological N0 and pathological N2 groups. Occult N2 lymph node metastasis was significantly associated with smoking history (OR = 1.693, $p = 0.020$), tumor maximum diameter (OR = 1.117, $p < 0.001$), density (OR = 0.146, $p < 0.001$), lobulation (OR = 42.066, $p < 0.001$), spiculation (OR = 6.177, $p < 0.001$), pleural indentation (OR = 4.377, $p < 0.001$), vascular cluster sign (OR = 2.376, $p = 0.003$), vacuole (OR = 2.367, $p < 0.001$), lepidic pattern (OR = 0.185, $p < 0.001$), acinar pattern (OR = 3.322, $p < 0.001$), micropapillary pattern (OR = 4.892, $p < 0.001$), solid pattern (OR = 8.850, $p < 0.001$), cribriform pattern (OR = 5.625,

Table 2 Univariate analysis of predictors of occult lymph node metastasis in clinical T1 lung adenocarcinoma

Variables	pN1 + N2			pN2		
	OR	95% CI	*p*-value	OR	95% CI	*p*-value
Age (years)[a]	0.995	0.979–1.011	0.555	0.999	0.980–1.019	0.917
Gender						
Male	1.000			1.000		
Female	0.719	0.517–1.001	0.050	0.745	0.503–1.104	0.142
Smoking history						
No	1.000			1.000		
Yes	1.891	1.308–2.734	<0.001*	1.693	1.086–2.641	0.020*
Maximum diameter (mm)[a]	1.129	1.097–1.163	<0.001*	1.117	1.080–1.155	<0.001*
Density						
Solid	1.000			1.000		
Part solid	0.116	0.063–0.212	<0.001*	0.146	0.075–0.286	<0.001*
GGO	0.000	0.000-∞	0.993	0.000	0.000-∞	0.993
Location						
Central	1.000			1.000		
Peripheral	0.171	0.011–2.749	0.213	0.114	0.007–1.842	0.126
Lung lobes						
LLL	1.000			1.000		
LUL	0.565	0.316–1.011	0.055	0.495	0.246–0.996	0.050
RUL	0.970	0.592–1.589	0.903	0.963	0.543–2.358	0.896
RML	1.292	0.693–2.407	0.420	1.119	0.531–2.358	0.767
RLL	1.220	0.717–2.075	0.464	1.095	0.585–2.048	0.777
Lobulation						
Absent	1.000			1.000		
Present	47.179	17.358-128.237	<0.001*	42.066	13.267–133.380	<0.001*
Spiculation						
Absent	1.000			1.000		
Present	6.762	4.706–9.716	<0.001*	6.177	4.041–9.443	<0.001*
Pleural indentation						
Absent	1.000			1.000		
Present	4.605	3.201–6.626	<0.001*	4.377	2.846–6.730	<0.001*
Air bronchogram						
Absent	1.000			1.000		
Present	1.079	0.759–1.534	0.671	0.864	0.559–1.336	0.512
Vascular cluster sign						
Absent	1.000			1.000		
Present	2.791	1.744–4.466	<0.001*	2.376	1.341–4.210	0.003*
Vacuole						
Absent	1.000			1.000		
Present	2.190	1.502–3.195	<0.001*	2.367	1.527–3.670	<0.001*
Lepidic pattern						
Absent	1.000			1.000		
Present	0.214	0.147–0.312	<0.001*	0.185	0.116–0.296	<0.001*
Acinar pattern						
Absent	1.000			1.000		
Present	2.516	1.558–4.062	<0.001*	3.322	1.755–6.291	<0.001*
Papillary pattern						
Absent	1.000			1.000		
Present	1.483	1.063–2.069	0.020*	1.444	0.972–2.145	0.069
Micropapillary pattern						
Absent	1.000			1.000		
Present	4.895	3.470–6.906	<0.001*	4.892	3.264–7.332	<0.001*
Solid pattern						

Table 2 (continued)

Variables	pN1 + N2			pN2		
	OR	95% CI	*p*-value	OR	95% CI	*p*-value
Absent	1.000			1.000		
Present	6.885	4.794–9.889	<0.001*	8.850	5.813–13.473	<0.001*
Complex glandular pattern						
Absent	1.000			1.000		
Present	1.842	0.666–5.098	0.239	2.211	0.726–6.732	0.163
Cribriform pattern						
Absent	1.000			1.000		
Present	5.266	1.884–14.723	0.002*	5.625	1.808–17.501	0.003*
Predominant pattern						
Lepidic predominant	1.000			1.000		
Acinar predominant	9.798	4.477–21.443	<0.001*	11.885	4.278–33.025	<0.001*
Papillary predominant	7.101	3.020-16.696	<0.001*	5.735	1.822–18.053	0.003*
Micropapillary predominant	37.143	12.789-107.877	<0.001*	48.750	13.466-176.482	<0.001*
Solid predominant	38.304	15.900-92.275	<0.001*	50.781	16.813-153.379	<0.001*
Complex glandular predominant	11.607	1.146-117.603	0.038*	20.312	1.837-224.562	0.014*
Visceral pleural invasion						
Absent	1.000			1.000		
Present	2.835	2.008–4.003	<0.001*	2.542	1.687–3.831	<0.001*
Perineural invasion						
Absent	1.000			1.000		
Present	9.023	3.793–21.468	<0.001*	7.126	2.600-19.527	<0.001*
Lymphovascular invasion						
Absent	1.000			1.000		
Present	9.668	6.530-14.315	<0.001*	9.111	5.815–14.276	<0.001*
STAS						
Absent	1.000			1.000		
Present	7.320	5.119–10.466	<0.001*	6.652	4.389–10.084	<0.001*
Emphysema						
Absent	1.000			1.000		
Present	1.050	0.746–1.479	0.779	1.040	0.692–1.565	0.849
ALK (D5F3 Ventana)						
Negative	1.000			1.000		
Positive	4.221	2.369–7.519	<0.001*	6.379	3.507–11.604	<0.001*
CYFRA21-1 (ng/ml)						
≤ 3.3	1.000			1.000		
> 3.3	1.265	0.663–2.414	0.476	1.428	0.686–2.971	0.341
CEA (ng/ml)						
< 5	1.000			1.000		
5–20	2.987	1.754–5.086	<0.001*	4.054	2.287–7.184	<0.001*
> 20	15.003	5.606–40.150	<0.001*	16.321	5.672–46.963	<0.001*
CA125 (U/mL)						
< 35	1.000			1.000		
≥ 35	2.930	1.442–5.952	0.003*	4.121	1.970–8.622	<0.001*

Abbreviations: RUL, right upper lobe; RML, right middle lobe; RLL, right lower lobe; LUL, left upper lobe; LLL, left lower lobe; STAS, spread through air space; *ALK*, anaplastic lymphoma kinase; Cyfra21-1, cytokeratin 19-fragments; CEA, carcinoembryonic antigen; CA125, carcinoma antigen 125. * Represents $p < 0.05$

[a] The data are the median, and the upper and lower interquartile ranges are in brackets

$p = 0.003$, predominant pattern (OR = 1.887, $p < 0.001$), visceral pleural invasion (OR = 2.542, $p < 0.001$), perineural invasion (OR = 7.126, $p < 0.001$), lymphovascular invasion (OR = 9.111, $p < 0.001$), STAS(OR = 6.652, $p < 0.001$), *ALK* (OR = 6.379, $p < 0.001$), CEA (OR = 4.046, $p < 0.001$), CA125 (OR = 4.121, $p < 0.001$). Multivariate logistic regression analysis showed that lobulation (OR = 11.533, $p < 0.001$), lymphovascular invasion (OR = 2.752, $p < 0.001$), STAS (OR = 1.850, $p = 0.027$), micropapillary pattern (OR = 2.181, $p = 0.004$), solid pattern (OR = 3.579,

Table 3 Multivariate analysis of predictors of occult lymph node metastasis in clinical T1 lung adenocarcinoma

Variables	pN1 + N2			pN2		
	OR	95% CI	*P*-value	OR	95% CI	*P*-value
Smoking history	0.968	0.595–1.574	0.895	0.870	0.493–1.535	0.630
Maximum diameter (mm)[a]	1.013	0.971–1.058	0.549	1.001	0.952–1.052	0.969
Density	0.379	0.197–0.729	0.004*	0.534	0.264–1.082	0.082
Lobulation	11.083	3.752–32.739	<0.001*	11.533	3.270-40.674	<0.001*
Spiculation	1.638	1.012–2.652	0.045*	1.462	0.836–2.557	0.183
Pleural indentation	1.586	0.957–2.629	0.073	1.652	0.912–2.992	0.097
Vascular cluster sign	1.091	0.604–1.972	0.772	0.983	0.486–1.985	0.961
Vacuole	1.284	0.785-2.100	0.320	1.514	0.863–2.655	0.148
Lepidic pattern	0.578	0.351–0.950	0.031*	0.512	0.282–0.928	0.027*
Acinar pattern	1.249	0.634–2.461	0.521	2.107	0.886–5.009	0.092
Papillary pattern	0.722	0.447–1.165	0.182			
Micropapillary pattern	2.222	1.397–3.535	0.001*	2.181	1.282–3.713	0.004*
Solid pattern	2.681	1.589–4.525	<0.001*	3.579	2.004–6.391	<0.001*
Cribriform pattern	1.102	0.304–3.996	0.883	0.900	0.214–3.777	0.885
Predominant pattern	0.973	0.786–1.204	0.803	1.009	0.795–1.281	0.939
Visceral pleural invasion	0.956	0.604–1.512	0.847	0.891	0.521–1.524	0.673
Perineural invasion	1.781	0.655–4.841	0.258	1.376	0.403–4.698	0.610
Lymphovascular invasion	2.969	1.820–4.841	<0.001*	2.752	1.562–4.850	<0.001*
STAS	2.280	1.440–3.609	<0.001*	1.850	1.074–3.186	0.027*
ALK (D5F3 Ventana)	1.892	0.838–4.272	0.125	2.748	1.198–6.305	0.017*
CEA (ng/ml)	1.702	1.055–2.747	0.029*	2.051	1.200-3.504	0.009*
CA125 (U/mL)	2.044	0.664–6.287	0.212	2.605	0.808–8.403	0.109

Abbreviations: 95% CI, 95% confidence interval; OR, odds ratio; STAS, spread through air space; *ALK*, anaplastic lymphoma kinase; CEA, carcinoembryonic antigen; CA125, carcinoma antigen 125. * Represents $p < 0.05$

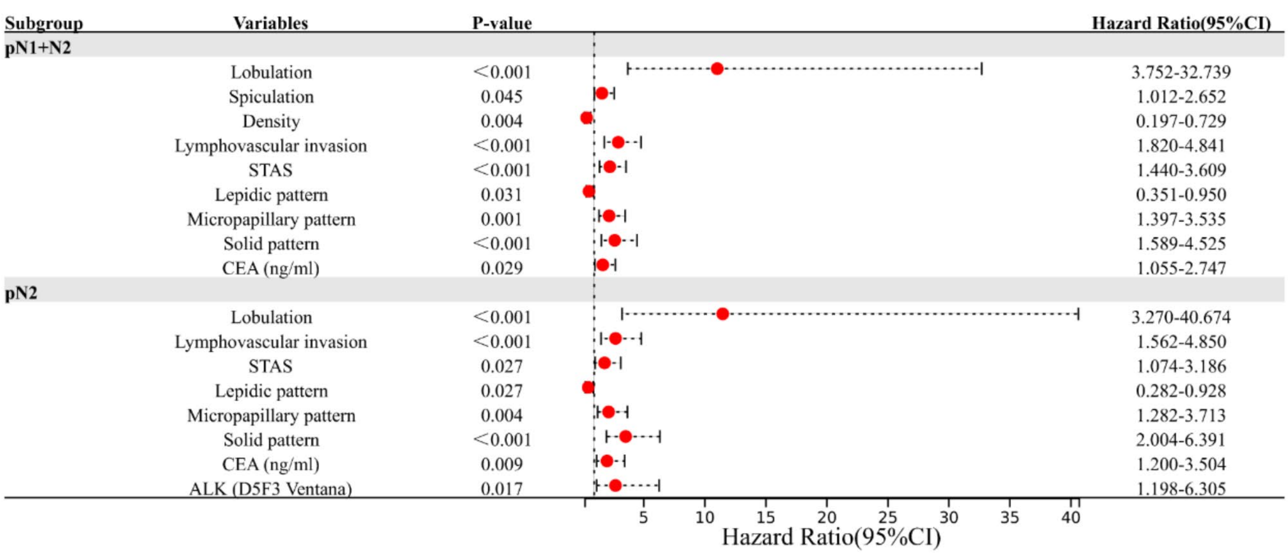

Fig. 1 The forest plot of multivariate logistic regression analysis shows the association between various predictive factors and pN1 + N2 as well as pN2. The horizontal lines represent the 95% confidence intervals (CI), and the red dots indicate the odds ratios (OR). A *P*-value of less than 0.05 was considered statistically significant

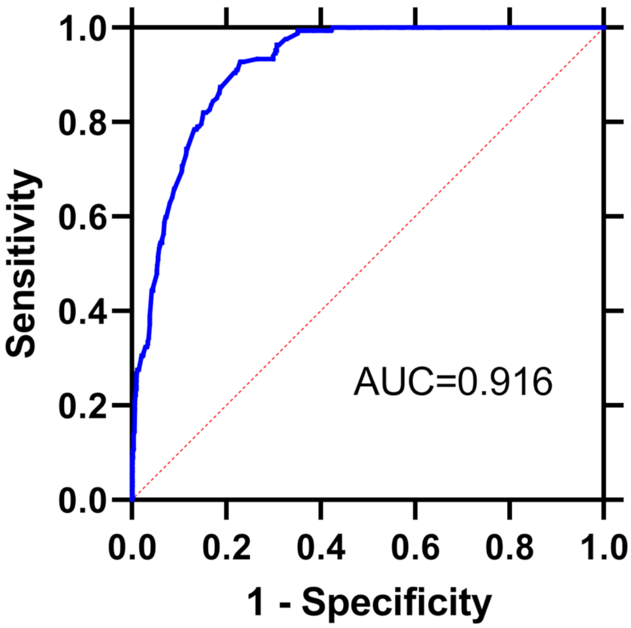

Fig. 2 Receiver operating characteristic curve (ROC) for predicting OLNM. By combining nine factors (lobulation, spiculation, density, lymphovascular invasion, STAS, lepidic pattern, micropapillary pattern, solid pattern, CEA), OLNM could be predicted. The sensitivity was 92.8%, the specificity was 77.0%, and the area under the curve (AUC) was 0.916

$p<0.001$), CEA (OR = 2.051, $p=0.009$), *ALK* (OR = 2.748, $p=0.017$) were identified as independent predictor associated with an increased risk of occult N2 lymph node metastasis. Conversely, the lepidic pattern (OR = 0.512, $p=0.027$) was an independent predictor associated with a decreased risk of occult N2 lymph node metastasis (Table 3; Fig. 1).

Discussion

Lymph node metastasis is an early event in the progression of lung cancer and is not uncommon even in tumors with a low clinical stage. According to the literature, the incidence of lymph node upstaging in patients with clinical stage I NSCLC who have undergone both radical surgery and lymph node dissection ranges from 10–35% [11, 16–19]. In this study, 167 (14.7%) patients with T1 lung adenocarcinoma were upstaged to pN1 or pN2 after anatomic resection. Despite the widespread use of conventional CT and PET/CT, accurate lymph node staging remains challenging. Therefore, identifying OLNM is critical to support treatment strategies for patients with clinical T1 lung adenocarcinoma, ensuring timely treatment and avoiding delays and overtreatment.

Thus, in this retrospective study, we conducted a comprehensive analysis of the clinicopathological characteristics and CT features of all patients. First, our findings confirmed that CEA was a risk factor for lymph node metastasis, which is consistent with previous studies [20, 21]. This underscores the importance of CEA in assessing the likelihood of lymph node involvement in lung adenocarcinoma patients. Consequently, surgeons should exercise increased caution when performing lymph node dissection in lung adenocarcinoma patients with elevated serum CEA levels. Second, our study demonstrated that solid nodules are more prone to OLNM than part-solid nodules. Consistent with our findings, Xiao et al. [22] reviewed 196 patients diagnosed with cT1N0M0 stage lung adenocarcinoma and identified solid nodules as a significant risk factor for lymph node metastasis. Furthermore, additional studies have corroborated these findings, indicating that a higher proportion of the solid component in part-solid adenocarcinomas is significantly associated with an increased likelihood of lymph node metastasis [23, 24]. Additionally, we observed that clinical T1 lung adenocarcinoma presenting as GGO on CT scans seldom exhibited OLNM, aligning with the findings of Wang et al. [25]. Specifically, solids nodules exhibit a higher propensity for lymph node metastasis, potentially due to their histological characteristics. As the solid component of the tumor increases, the proportion of lepidic components decreases, with acinar, micropapillary, and solid structures becoming more prominent. This shift is associated with increased local invasiveness and a higher likelihood of lymphatic invasion [26]. Third, our analysis revealed that tumor size does not have a significant effect on lymph node metastasis in lung adenocarcinoma patients, which aligns with the findings of several other studies [11, 25, 27]. However, contrasting evidence exists, as some studies have reported that the incidence of lymph node metastasis increased with tumor size [17, 28, 29]. Moreover, some studies have suggested that the risk of lymph node metastasis correlates more strongly with the size of the solid portion of the tumor rather than the overall tumor size [23, 30]. Given that our study included GGO nodules, which generally exhibit a lower metastatic potential, this could explain the discrepancy in results observed between our study and others.

Regarding CT features, our study found that lobulation and spiculation were significantly associated with a higher risk of OLNM, and that lobulation was significantly associated with occult N2 lymph node metastasis. In 2023, Zhao et al. [31] similarly identified lobulation as an independent predictor of OLNM in clinical IA-IIA lung adenocarcinoma. Likewise, Li et al. [32] reported that spiculation served as an independent risk factor for predicting lymph node metastasis in patients with peripheral lung adenocarcinoma. In contrast, He et al. [33] did not observe any significant association between lobulation, spiculation, and OLNM in peripheral non-small cell carcinoma. Furthermore, previous studies identified Type II pleural involvement — defined as a single linear or cord-like pleural tag, or a tumor abutting the pleura with a broad base (visible on both lung and mediastinal window images) — as an independent predictive factor for OLNM [33]. This finding does not align with our results, which did not demonstrate an association between pleural indentation and OLNM. Such discrepancies may be attributed to differences in inclusion and exclusion criteria among studies. For instance, our study population may have included a higher proportion of early-stage lung adenocarcinoma cases, in which pleural involvement is less pronounced, thereby reducing its predictive value for OLNM. Additionally, we found no association between the presence of an air bronchogram and OLNM in lung adenocarcinoma, consistent with the findings of Yoshino et al. [34]. Lobulated margins reflect heterogeneous growth rates within different regions of the tumor [35]. This heterogeneity typically corresponds to enhanced cellular proliferation and increased angiogenesis, thereby promoting elevated invasiveness and metastatic potential [36]. As a result, the tumor more readily breaches its primary boundaries, invades surrounding tissues, and disseminates via lymphatic channels to regional lymph nodes, increasing the likelihood of lymphatic spread. Pathological investigations have shown that spiculation can be attributed to thickened interlobular septa, fibrosis arising from the obstruction of peripheral vessels, or lymphatic channels filled with tumor cells [37]. Consequently, the infiltration of tumor cells into lymphatic channels not only contributes to the formation of spiculated contours but also facilitates nodal dissemination. These insights may prove valuable in predicting OLNM in clinical T1 lung adenocarcinoma.

Molecular testing has been widely adopted in clinical practice, serving not only to guide targeted drug therapy but also to aid in prognosis prediction and patient characterization. Patients with positive *ALK* expression tend to be diagnosed at a relatively advanced stage, often presenting with nodal and distant metastasis [38, 39]. However, the incidence of *ALK* alterations in early-stage NSCLC ranges from 2–7% [40]. In this study, 53 (4.7%) patients with T1 lung adenocarcinoma exhibited positive *ALK* expression. We found a significant correlation between *ALK* positivity and occult N2 lymph node metastasis. Similarly, Seto et al. demonstrated that *ALK* rearrangements were significantly associated with a higher incidence of OLNM compared to *ALK*-negative adenocarcinomas [14]. Furthermore, studies have shown that lung adenocarcinoma patients with *ALK* rearrangement have a poorer prognosis compared to those with wild-type *ALK* [41, 42]. Additionally, *ALK* rearrangements are more frequently observed in patients with poorly differentiated lung adenocarcinoma [43]. Therefore, *ALK* positivity may serve as an important prognostic indicator for predicting OLNM in clinical T1 lung adenocarcinoma. Based on these findings, we hypothesize that performing radical resection in T1 lung adenocarcinomas with *ALK* positivity may provide a curative opportunity.

In terms of pathology, lymphovascular invasion often indicates early lymph node metastasis and suggests a poor prognosis [44, 45]. Our study confirmed that lymphovascular invasion significantly increases the risk of OLNM. The relationship between visceral pleural infiltration and lymph node metastasis remains controversial [6, 11, 44], and it was not associated with OLNM in our study. Moreover, the literature suggested that lymph node metastasis in lung adenocarcinoma patients with tumor ≤ 3 cm varies by histological subtype [46]. Specifically, solid and micropapillary patterns are significantly more likely to involve lymph nodes than other subtypes [47]. Consistent with these findings, our study demonstrated that micropapillary and solid patterns are significantly associated with both OLNM and occult N2 lymph node metastasis. Furthermore, STAS has been recognized as a novel invasion mechanism, crucial for pathologists' understanding of tumor behavior. In our study, STAS significantly increased the risk of OLNM in clinical T1 lung adenocarcinoma, consistent with the finding of Vaghjiani et al. [48]. There is considerable evidence that STAS is associated with lower survival rates and acts as an independent prognostic factor, regardless of tumor stage [49, 50]. Travis et al. [51] have suggested introducing STAS as a histological descriptor in the 9th edition of the TNM classification for lung cancer. Accurate preoperative identification of STAS by pathologists could serve as a crucial reference for selecting the optimal surgical approach and improving patient prognosis. Additionally, our results demonstrated that the lepidic pattern was an independent protective factor against OLNM, with a significantly lower risk of metastasis (OR = 0.578, 95% CI:0.351–0.950). Zhang et al. [52] through a multicenter prospective clinical trial, found that the lepidic subtype of lung adenocarcinoma has a 94.0% accuracy rate in predicting negative lymph node status. The presence of the lepidic component could enhance prognosis prediction in patients with T1 lung adenocarcinoma [53].

This study has several limitations that should be acknowledged. First, its retrospective design may introduce selection bias, potentially affecting the generalizability of the findings. While the inclusion of a two-centered sample enhances the representativeness of the results, the inherent constraints of retrospective studies remain a limitation. Second, the absence of PET imaging as a staging modality may have led to an overestimation of cT1N0 cases, potentially influencing the accuracy of preoperative staging. Third, the study specifically focused on patients with T1 lung adenocarcinoma and lacked long-term follow-up data, which limited the ability to evaluate the relationship between OLNM and survival outcomes. Future studies incorporating survival analysis are essential for a more comprehensive assessment of prognosis. Additionally, the relatively small number of OLNM cases in the sample reduced the statistical power of the findings. Larger-scale studies with prospective designs are necessary to validate and generalize these results, providing stronger evidence to guide clinical practice.

Conclusion

In conclusion, our study identified several independent predictors for OLNM and occult N2 lymph node metastasis in clinical T1 lung adenocarcinoma, including lobulation, spiculation, density, lymphovascular invasion, STAS, lepidic pattern, micropapillary pattern, solid pattern, CEA, and *ALK*. These predictive factors may assist clinicians in assessing the risk of OLNM in clinical T1 lung adenocarcinoma, potentially informing more targeted intervention strategies.

Abbreviations

95% CI	95% confidence interval
ALK	Anaplastic lymphoma kinase
AUC	The area under the receiver
CA125	Carcinoma antigen 125
CEA	Carcinoembryonic antigen
CT	Computed tomography
CYFRA21-1	Cytokeratin 19-fragments
GGO	Ground-glass opacity
LLL	Left lower lobe
LUL	Left upper lobe
NSCLC	Non-small cell lung cancer
OLNM	Occult lymph node metastasis
OR	Odds ratio
PET/CT	Positron emission tomography/computed tomography
RLL	Right lower lobe
RML	Right middle lobe
RUL	Right upper lobe
STAS	Spread through air spaces

Acknowledgements

The authors wish to express their gratitude to all the patients, nurses, and physicians who contributed to and participated in this study.

Author contributions

XXH1 and GQJ contributed to the conception and design of the study. Data collection was carried out collaboratively by XXH1, XXH2, and KW. XXH1 performed the data analysis and interpretation of the results. XXH1, LJL, and GQJ participated in the critical revision, data curation, and review of the final manuscript, which was approved by all authors. XXH1 refers to Xiaoxin Huang. XXH2 refers to Xiaoxiao Huang.

Funding

This work was supported by Beijing Medical Award Foundation (< grant number YXJL-2022-0665-0210>[to < Guanqiao Jin>]); Guangxi Key Research & Development Program (< grant number AB2323026087>[to < Guanqiao Jin>]); and Guangxi Natural Science Foundation (< grant number 2023GXNSFAA026225>[to < Guanqiao Jin>]).

Data availability

All data generated or analysed during this study are included in this published article.

Declarations

Ethics approval and consent to participate

The ethics committee of Guangxi Medical University Cancer Hospital approved the retrospective study and waived informed consent [NO. KY-2022-301].

Consent for publication

Not applicable.

Competing interests

The authors declare no competing interests.

Received: 25 September 2024 / Accepted: 17 February 2025

Published online: 01 March 2025

References

1. Bray F, Laversanne M, Sung H, Ferlay J, Siegel RL, Soerjomataram I, et al. Global cancer statistics 2022: GLOBOCAN estimates of incidence and mortality worldwide for 36 cancers in 185 countries. Cancer J Clin. 2022;74(3):229–63. https://doi.org/10.3322/caac.21834
2. Siegel RL, Miller KD, Fuchs HE, Jemal A. Cancer statistics. 2022. CA: A Cancer Journal for Clinicians. 2022;72(1):7–33. https://doi.org/10.3322/caac.21708
3. Howington JA, Blum MG, Chang AC, Balekian AA, Murthy SC. Treatment of stage I and II non-small cell lung cancer. Chest. 2013;143(5):eS278–e313. https://doi.org/10.1378/chest.12-2359
4. Fréchet B, Kazakov J, Thiffault V, Ferraro P, Liberman M. Diagnostic accuracy of mediastinal lymph node staging techniques in the preoperative assessment of nonsmall cell lung cancer patients. J Bronchol Interventional Pulmonol. 2018;25(1):17–24. https://doi.org/10.1097/LBR.0000000000000425
5. Terumoto Koike TK, Yasushi Yamato K, Yoshiya, Shin-ichi Toyabe. Predictive risk factors for mediastinal lymph node metastasis in clinical stage IA non-small-cell lung cancer patients. J Thorac Oncol. 2012;7(8):1246–51. https://doi.org/10.1097/JTO.0b013e31825871de
6. Fang C, Xiang Y, Han W. Preoperative risk factors of lymph node metastasis in clinical N0 lung adenocarcinoma of 3 cm or less in diameter. BMC Surg. 2022;22(1). https://doi.org/10.1186/s12893-022-01605-z
7. Zhang W, Mu G, Huang J, Bian C, Wang H, Gu Y, et al. Lymph node metastasis and its risk factors in T1 lung adenocarcinoma. Thorac Cancer. 2023;14(30):2993–3000. https://doi.org/10.1111/1759-7714.15088
8. Koike T, Koike T, Yamato Y, Yoshiya K, Toyabe S-i. Predictive risk factors for mediastinal lymph node metastasis in clinical stage IA non–small-cell lung cancer patients. J Thorac Oncol. 2012;7(8):1246–51. https://doi.org/10.1097/JTO.0b013e31825871de
9. Kanzaki R, Higashiyama M, Fujiwara A, Tokunaga T, Maeda J, Okami J, et al. Occult mediastinal lymph node metastasis in NSCLC patients diagnosed as clinical N0-1 by preoperative integrated FDG-PET/CT and CT: risk factors, pattern, and histopathological study. Lung Cancer. 2011;71(3):333–7. https://doi.org/10.1016/j.lungcan.2010.06.008
10. Nitadori J-i, Bograd AJ, Kadota K, Sima CS, Rizk NP, Morales EA, et al. Impact of micropapillary histologic subtype in selecting limited resection vs lobectomy for lung adenocarcinoma of 2 cm or smaller. JNCI: J Natl Cancer Inst. 2013;105(16):1212–20. https://doi.org/10.1093/jnci/djt166
11. Hung J-J, Yeh Y-C, Jeng W-J, Wu Y-C, Chou T-Y, Hsu W-H. Factors predicting occult lymph node metastasis in completely resected lung adenocarcinoma of 3 cm or smaller. Eur J Cardiothorac Surg. 2016;50(2):329–36. https://doi.org/10.1093/ejcts/ezv485
12. Lee H-S, Liu J, Li J, Lin G, Long Z, Li Q, et al. Risk factors of lobar lymph node metastases in non-primary tumor-bearing lobes among the patients of non-small-cell lung cancer. PLoS ONE. 2020;15(9):e0239281. https://doi.org/10.1371/journal.pone.0239281
13. Gallina FT, Tajè R, Letizia Cecere F, Forcella D, Landi L, Minuti G, et al. ALK rearrangement is an independent predictive factor of unexpected nodal metastasis after surgery in early stage, clinical node negative lung adenocarcinoma. Lung Cancer. 2023;180:107215. https://doi.org/10.1016/j.lungcan.2023.107215
14. Seto K, Kuroda H, Yoshida T, Sakata S, Mizuno T, Sakakura N, et al. Higher frequency of occult lymph node metastasis in clinical N0 pulmonary adenocarcinoma with ALK rearrangement. Cancer Manage Res. 2018;10:2117–24. https://doi.org/10.2147/CMAR.S147569

15. Lardinois D, Deleyn P, Vanschil P, Porta R, Waller D, Passlick B, et al. ESTS guidelines for intraoperative lymph node staging in non-small cell lung cancer☆. Eur J Cardiothorac Surg. 2006;30(5):787–92. https://doi.org/10.1016/j.ejcts.2006.08.008
16. Licht PB, Jørgensen OD, Ladegaard L, Jakobsen E. A national study of nodal upstaging after thoracoscopic versus open lobectomy for clinical stage I lung cancer. Ann Thorac Surg. 2013;96(3):943–50. https://doi.org/10.1016/j.athoracsur.2013.04.011
17. Kaseda K, Asakura K, Kazama A, Ozawa Y. Risk factors for predicting occult lymph node metastasis in patients with clinical stage I non-small cell lung cancer staged by integrated fluorodeoxyglucose positron emission tomography/computed tomography. World J Surg. 2016;40(12):2976–83. https://doi.org/10.1007/s00268-016-3652-5
18. Ghaly G, Rahouma M, Kamel MK, Nasar A, Harrison S, Nguyen AB, et al. Clinical predictors of nodal metastases in peripherally clinical T1a N0 non-small cell lung cancer. Ann Thorac Surg. 2017;104(4):1153–8. https://doi.org/10.1016/j.athoracsur.2017.02.074
19. Tian W, Yan Q, Huang X, Feng R, Shan F, Geng D, et al. Predicting occult lymph node metastasis in solid-predominantly invasive lung adenocarcinoma across multiple centers using radiomics-deep learning fusion model. Cancer Imaging. 2024;24(1). https://doi.org/10.1186/s40644-024-00654-2
20. Sun G, Sun Y, Zou Z, Xu S. Analysis of segmental lymph node metastasis and clinical features in cT1N0M0 lung adenocarcinoma. Biomed Res Int. 2020;2020:1–7. https://doi.org/10.1155/2020/2842604
21. Gu Y, She Y, Xie D, Dai C, Ren Y, Fan Z, et al. A texture analysis–based prediction model for lymph node metastasis in stage IA lung adenocarcinoma. Ann Thorac Surg. 2018;106(1):214–20. https://doi.org/10.1016/j.athoracsur.2018.02.026
22. Xiao F, Yu Q, Zhang Z, Liu D, Guo Y, Liang C, et al. Novel perspective to evaluate the safety of segmentectomy: clinical significance of lobar and segmental lymph node metastasis in cT1N0M0 lung adenocarcinoma†. Eur J Cardiothorac Surg. 2018;53(1):228–34. https://doi.org/10.1093/ejcts/ezx263
23. Li W, Zhou F, Wan Z, Li M, Zhang Y, Bao X, et al. Clinicopathologic features and lymph node metastatic characteristics in patients with adenocarcinoma manifesting as part-solid nodule exceeding 3 cm in diameter. Lung Cancer. 2019;136:37–44. https://doi.org/10.1016/j.lungcan.2019.07.029
24. Lee SY, Jeon JH, Jung W, Chae M, Hwang WJ, Hwang Y, et al. Predictive factors for lymph node metastasis in clinical stage I part-solid lung adenocarcinoma. Ann Thorac Surg. 2021;111(2):456–62. https://doi.org/10.1016/j.athoracsur.2020.05.083
25. Wang Y, Jing L, Wang G. Risk factors for lymph node metastasis and surgical methods in patients with early-stage peripheral lung adenocarcinoma presenting as ground glass opacity. J Cardiothorac Surg. 2020;15(1):121. https://doi.org/10.1186/s13019-020-01167-2
26. Moon YKK, Sung SW, Lee KY, Kim YK, Kang JH, Kim YS, Park JK. Correlation of histological components with tumor invasion in pulmonary adenocarcinoma. World J Surg Oncol. 2014;12:388. https://doi.org/10.1186/1477-7819-12-388
27. Ouyang M-l, Xia H-w, Xu M-m, Lin J, Wang L-l, Zheng X-w, et al. Prediction of occult lymph node metastasis using SUV, volumetric parameters and intratumoral heterogeneity of the primary tumor in T1-2N0M0 lung cancer patients staged by PET/CT. Ann Nucl Med. 2019;33(9):671–80. https://doi.org/10.1007/s12149-019-01375-4
28. Wang K, Xue M, Qiu J, Liu L, Wang Y, Li R, et al. Genomics analysis and nomogram risk prediction of occult lymph node metastasis in non-predominant micropapillary component of lung adenocarcinoma measuring ≤ 3 cm. Front Oncol. 2022;12:945997. https://doi.org/10.3389/fonc.2022.945997
29. Li F, Zhai S, Fu L, Yang L, Mao Y. Nomograms for intraoperative prediction of lymph node metastasis in clinical stage IA lung adenocarcinoma. Cancer Med. 2023;12(13):14360–74. https://doi.org/10.1002/cam4.6115
30. Tsutani Y, Miyata Y, Nakayama H, Okumura S, Adachi S, Yoshimura M, et al. Prognostic significance of using solid versus whole tumor size on high-resolution computed tomography for predicting pathologic malignant grade of tumors in clinical stage IA lung adenocarcinoma: a multicenter study. J Thorac Cardiovasc Surg. 2012;143(3):607–12. https://doi.org/10.1016/j.jtcvs.2011.10.037
31. Zhao F, Zhao Y, Zhang Y, Sun H, Ye Z, Zhou G. Predictability and utility of contrast-enhanced ct on occult lymph node metastasis for patients with clinical stage IA-IIA lung adenocarcinoma: a double-center study. Acad Radiol. 2023;30(12):2870–9. https://doi.org/10.1016/j.acra.2023.03.002
32. Li Q, He X-q, Fan X, Zhu C-n, Lv J-w, Luo T-y. Development and validation of a combined model for preoperative prediction of lymph node metastasis in peripheral lung adenocarcinoma. Front Oncol. 2021;11:675877. https://doi.org/10.3389/fonc.2021.675877
33. He X-Q, Luo T-Y, Li X, Huo J-W, Gong J-W, Li Q. Clinicopathological and computed tomographic features associated with occult lymph node metastasis in patients with peripheral solid non-small cell lung cancer. Eur J Radiol. 2021;144:109981. https://doi.org/10.1016/j.ejrad.2021.109981
34. Yoshino IIY, Nagashima A, Takeo S, Motohiro A, Yano T, Yokoyama H, Ueda H, Sugio K, Ishida T, Yasumoto K, Maehara Y, Kyushu Lung Cancer Surgery Cooperative Group. Clinical characterization of node-negative lung adenocarcinoma: results of a prospective investigation. J Thorac Oncol. 2006;1(8):825–31. https://doi.org/10.1016/S1556-0864(15)30412-3
35. Rosado-de-Christenson MLTP, Moran CA. Bronchogenic carcinoma: radiologic-pathologic correlation. Radiographics: Rev publication Radiological Soc North Am. 1994;14(2):429–48. https://doi.org/10.1148/radiographics.14.2.8190965
36. Yang XYH, Liu H, Xie Y, Hu M. Vascular manifestations of small solitary pulmonary masses. Angiographic-pathologic correlations and clinical significance. Invest Radiol. 1996;31(5):275–9. https://doi.org/10.1097/00004424-199605000-00005
37. Kuriyama K TR, Doi, O, Kodama K, Tatsuta M, Matsuda M, Mitani T, Narumi Y, Fujita M. CT-pathologic correlation in small peripheral lung cancers. AJR Am J Roentgenol. 1987;149(6):1139–43. https://doi.org/10.2214/ajr.149.6.1139
38. Choi Y, Kim K-H, Jeong B-H, Lee K-J, Kim H, Kwon OJ, et al. Clinicoradiopathological features and prognosis according to genomic alterations in patients with resected lung adenocarcinoma. J Thorac Disease. 2020;12(10):5357–68. https://doi.org/10.21037/jtd-20-1716
39. Wang H, Wang Z, Zhang G, Zhang M, Zhang X, Li H, et al. Driver genes as predictive indicators of brain metastasis in patients with advanced NSCLC: EGFR, ALK, and RET gene mutations. Cancer Med. 2019;9(2):487–95. https://doi.org/10.1002/cam4.2706
40. Chen MF, Chaft JE. Early-stage ALK-positive lung cancer: a narrative review. Translational Lung Cancer Res. 2023;12(2):337–45. https://doi.org/10.21037/tlcr-22-631
41. Zhu J, Wang W, Xiong Y, Xu S, Chen J, Wen M, et al. Evolution of lung adenocarcinoma from preneoplasia to invasive adenocarcinoma. Cancer Med. 2022;12(5):5545–57. https://doi.org/10.1002/cam4.5393
42. Kim MH, Shim HS, Kang DR, Jung JY, Lee CY, Kim DJ, et al. Clinical and prognostic implications of ALK and ROS1 rearrangements in never-smokers with surgically resected lung adenocarcinoma. Lung Cancer. 2014;83(3):389–95. https://doi.org/10.1016/j.lungcan.2014.01.003
43. Zhang SYB, Zheng J, Zhao J, Zhou J. Gene status and clinicopathologic characteristics of lung adenocarcinomas with mediastinal lymph node metastasis. Oncotarget. 2016;7(39):63758–66. https://doi.org/10.18632/oncotarget.11494
44. Liang S, Huang Y-Y, Liu X, Wu L-L, Hu Y, Ma G. Risk profiles and a concise prediction model for lymph node metastasis in patients with lung adenocarcinoma. J Cardiothorac Surg. 2023;18(1):195. https://doi.org/10.1186/s13019-023-02288-0
45. Moon Y, Choi SY, Park JK, Lee KY. Risk factors for occult lymph node metastasis in peripheral non-small cell lung cancer with invasive component size 3 cm or less. World J Surg. 2020;44(5):1658–65. https://doi.org/10.1007/s00268-019-05365-5
46. Yu Y, Jian H, Shen L, Zhu L, Lu S. Lymph node involvement influenced by lung adenocarcinoma subtypes in tumor size ≤ 3 cm disease: A study of 2268 cases. Eur J Surg Oncol (EJSO). 2016;42(11):1714–9. https://doi.org/10.1016/j.ejso.2016.02.247
47. Lin W, Huang M, Zhang Z, Chai T, Chen S, Gao L, et al. A retrospective study of the relationship between the pathologic subtype and lymph node metastasis of lung adenocarcinomas of ≤ 3 cm diameter. Medicine. 2020;99(36):e21453. https://doi.org/10.1097/MD.0000000000021453
48. Vaghjiani RG, Takahashi Y, Eguchi T, Lu S, Kameda K, Tano Z, et al. Tumor spread through air spaces is a predictor of occult lymph node metastasis in clinical stage IA lung adenocarcinoma. J Thorac Oncol. 2020;15(5):792–802. https://doi.org/10.1016/j.jtho.2020.01.008
49. Han YB, Kim H, Mino-Kenudson M, Cho S, Kwon HJ, Lee KR, et al. Tumor spread through air spaces (STAS): prognostic significance of grading in non-small cell lung cancer. Mod Pathol. 2021;34(3):549–61. https://doi.org/10.1038/s41379-020-00709-2
50. Fan LQJ, Lin X, Wu Y, He Z, He P. Analysis of clinicopathological features on spread through air spaces of lung adenocarcinoma. Zhongguo Fei Ai Za Zhi. 2023;26(9):650–8. https://doi.org/10.3779/j.issn.1009-3419.2023.106.18

51. Travis WD, Eisele M, Nishimura KK, Aly RG, Bertoglio P, Chou T-Y, et al. The International Association for the Study of Lung Cancer (IASLC) Staging Project for lung cancer: recommendation to introduce spread through air spaces as a histologic descriptor in the ninth edition of the TNM classification of lung cancer. Analysis of 4061 Pathologic Stage I NSCLC. J Thorac Oncol. 2024;19(7):1028–51. https://doi.org/10.1016/j.jtho.2024.03.015
52. Zhang Y, Deng C, Zheng Q, Qian B, Ma J, Zhang C, et al. Selective mediastinal lymph node dissection strategy for clinical t1n0 invasive lung cancer: a prospective, multicenter, clinical trial. J Thorac Oncol. 2023;18(7):931–9. https://doi.org/10.1016/j.jtho.2023.02.010
53. Zhu E, Dai C, Xie H, Su H, Hu X, Li M, et al. Lepidic component identifies a subgroup of lung adenocarcinoma with a distinctive prognosis: a multicenter propensity-matched analysis. Therapeutic Adv Med Oncol. 2020;12:175883592098284. https://doi.org/10.1177/1758835920982845

Publisher's note